

Off-axis beam angle dependence of intensity fluctuation

Masahiro Toyoda

National Institute of Information and Communications Technology
4-2-1 Nukuikita-machi, Koganei, Tokyo 184-8795, Japan, E-mail: toyoda@nict.go.jp

ABSTRACT

The variance in intensity of a laser beam propagating through a turbulent medium increases with the off-axis beam angle. Measurements of this dependence for an uplink qualitatively agreed with theory.

1. INTRODUCTION

Fluctuation in the intensity of the laser beam is a primary factor limiting the quality of wireless laser communication and thus the communication bandwidth. The intensity fluctuation must be stabilized for wireless laser communication to become practical. This fluctuation is due to either refractive index fluctuation along the path (atmospheric turbulence) or a pointing error in transmitting the laser beam. Given the limited emitting power of the laser, laser beam transmission with narrow divergence is necessary for communication between two distant terminals. Moreover, a technique is needed for accurately aiming the laser beam.

When fluctuation is due to atmospheric turbulence, the intensity variance at the receiving point increases with the distance from the center of the beam pattern to the receiving point. Here, we call the angle between the beam axis and the line from the transmitting point to the receiving point the “off-axis beam angle.” The relationship between the intensity variance and the off-axis beam angle has been investigated theoretically.¹⁻³ We used known theory to first investigate the off-axis beam angle dependences of the mean intensity and log-intensity variance for single-beam transmission. We then measured them in an actual uplink transmission to a satellite.

2. OFF-AXIS BEAM ANGLE DEPENDENCE OF INTENSITY FLUCTUATION

2.1 Mean intensity

When a light wave propagates in a turbulent medium, its wavefront phase and intensity distribution are perturbed. In this section, we use known theory to describe the off-axis beam angle dependence of the intensity variation when a beam wave propagates between the ground and a satellite (slant path). The scale size of a blob of turbulence is assumed to be fairly large in comparison with the wavelength of the beam. In addition, we assume that the state of the refractive index fluctuation is isotropic, the turbulence is weak, and the Rytov and Born approximations can be used to solve the wave equation.

Furthermore, the statistical condition of the refractive index fluctuation varies slowly along the slant path. We denote the distance from the center of the beam pattern to a point on the receiving plane as ρ and the propagation distance of the beam as L .

When the beam is emitted with a Gaussian intensity distribution, its time averaged intensity at received position (ρ, L) can be expressed as

$$\langle I(\rho, L) \rangle = \frac{W_0^2}{W_e(L)^2} \exp\left(-2 \frac{\rho^2}{W_e(L)^2}\right), \quad (1)$$

where $\langle \cdot \rangle$ means time averaging, W_0 is the beam radius at transmission, and $W_e(L)$ is the beam radius at reception.⁴ This $\langle I(\rho, L) \rangle$ is standardized by the intensity at the center of the beam at transmission. In addition, $W_e(L)$ can be expressed as

$$W_e(L) = W(L) \left\{ 1 + 4\pi^2 k^2 \times \int_0^L d\eta \int_0^\infty d\kappa \kappa \Phi_n(\eta, \kappa) \left\{ 1 - \exp\left[\frac{-2\kappa^2 (L-\eta)^2}{k^2 W(L)^2} \right] \right\} \right\}^{\frac{1}{2}}, \quad (2)$$

where k is the wave number of the beam, η is variable about the propagation distance, κ is the spatial wave number of the refractive index fluctuation, and $\Phi_n(\eta, \kappa)$ is the three-dimensional power spectrum of the refractive index fluctuation. Moreover, $W(L)$ is the beam radius at L in the absence of atmospheric turbulence:

$$W(L) = W_0 \left[\left(1 - \frac{L}{R_0} \right)^2 + \left(\frac{2L}{k W_0^2} \right)^2 \right]^{\frac{1}{2}}, \quad (3)$$

where R_0 is the radius of the curvature of the wavefront at the transmitting point; it is positive for a converging beam and negative for a diverging beam.⁴

Given Eq. (2), when the refractive index fluctuation takes the form of a Kolmogorov spectrum, the beam radius of the uplink is given by

$$W_{e, up}(L) = W(L) \left\{ 1 + 0.033 \times 4\pi^2 k_{up}^2 \sec \Theta \times \int_{H_0}^H dh \int_{\kappa_0}^{\kappa_{\max}} d\kappa \kappa^{-\frac{8}{3}} C_n^2(h) \left\{ 1 - \exp\left[\frac{-2\kappa^2 (H-h)^2}{k_{up}^2 W(L)^2 (\cos \Theta)^2} \right] \right\} \right\}^{\frac{1}{2}}, \quad (4)$$

where k_{up} is the wave number of the uplink, Θ is the zenith angle, H_0 is the altitude of the ground, H is the altitude of the satellite, and $L = (H - H_0) \sec \Theta$. In addition, $C_n^2(h)$ is the refractive index structure constant at altitude h . We denote $\kappa_{\max} = 2\pi/l_0$ and $\kappa_0 = 2\pi/L_0$,

where l_0 is the inner scale, i.e., the minimum size of a blob of turbulence, and L_0 is the outer scale, i.e., its maximum size.

Figure 1 shows the relationship between $\langle I(\rho, L) \rangle$ (normalized by the peak intensity of the unperturbed uplink) and the off-axis beam angle, ϕ , calculated using Eqs. (1)–(4) for atmospheric-perturbed and unperturbed uplinks. The curves represent the beam pattern at the satellite. We set beam parameter W_0 to 0.055 m and $1/R_0$ to 0 (collimated). The height in Eq. (4) was integrated up to an altitude of 20 km. In addition, we set v and A_{HV} in the H-V model of $C_n^2(h)$ to 24.6 m/s and $= 3 \times 10^{-13} \text{ m}^{-2/3}$, respectively, to make the calculated value of $W_{e, up}(L)$ about five times that of $W(L)$ for the uplink. Here, when L is fixed, $\phi \cong \rho/L$ and $\langle I(\rho, L) \rangle$ can be expressed by $\langle I(\rho, L) \rangle \cong \langle I(\phi) \rangle$. The model of $C_n^2(h)$ used in Eq. (4) is described in the appendix.

The beam radius for a downlink is expressed by

$$W_{e, down}(L) = W(L) \left\{ 1 + 0.033 \times 8\pi^2 k_d^2 \sec \Theta \times \int_{H_0}^H dh \int_{k_0}^{k_{\max}} d\kappa \kappa^{-\frac{8}{3}} C_n^2(h) \exp \left[\frac{-2\kappa^2}{k_d^2 W(L)^2} \left(\frac{h-H_0}{\cos \Theta} \right)^2 \right] \right\}^{\frac{1}{2}}, \quad (5)$$

where k_d is the wave number of the downlink. When we calculate Eq. (5), $W_{e, down}(L) \cong W(L)$ is obtained. Because the diameter of the downlink beam in the troposphere is large, $W_{e, down}(L)$ is close to that for the downlink in the absence of atmospheric turbulence.

2.2 Log-intensity variance

When the refractive index fluctuation takes the form of a Kolmogorov spectrum, the log-intensity variance of the uplink is expressed by

$$B_{I, up}(\rho, L) = 0.033 \times 8\pi^2 k_{up}^2 \sec \Theta \times \int_{H_0}^H dh \int_{k_0}^{k_{\max}} d\kappa \kappa^{-\frac{8}{3}} C_n^2(h) \exp \left[\frac{-\gamma_i \kappa^2 (H-h)}{k_{up} \cos \Theta} \right] \times \left\{ I_0(2\gamma_i \kappa \rho) - \cos \left[\frac{\gamma_r \kappa^2 (H-h)}{k_{up} \cos \Theta} \right] \right\}, \quad (6)$$

where $I_0(\cdot)$ is a modified Bessel function.⁴ In addition, γ_r and γ_i are real numbers, and

$$\gamma_r - i\gamma_i = \frac{1 + i \left(\frac{\lambda}{\pi W_0^2} + i \frac{1}{R_0} \right) \eta}{1 + i \left(\frac{\lambda}{\pi W_0^2} + i \frac{1}{R_0} \right) L}, \quad (7)$$

where λ is the wavelength. Figure 2 shows the calculated relationship between $B_{I, up}(\rho, L)$ and ϕ for a W_0 of 0.01, 0.02, and 0.055 m. The variation rate of $B_{I, up}(\rho, L)$ increased with W_0 . This off-axis beam angle dependence is similar to those calculated by Shelton² and by Andrews and Phillips.³ If L is fixed, $B_{I, up}(\rho, L)$ can be expressed as

$$B_{I, up}(\rho, L) = B_{I, up}(\phi).$$

If the averaging effect on the intensity fluctuation in the receiving telescope is not considered, the log-intensity variance of the downlink is given by

$$B_{I, down}(\rho, L) = 0.033 \times 8\pi^2 k_d^2 \sec \Theta \times \int_{H_0}^H dh \int_{k_0}^{k_{\max}} d\kappa \kappa^{-\frac{8}{3}} C_n^2(h) \exp \left[\frac{-\gamma_i \kappa^2 (h-H_0)}{k_d \cos \Theta} \right] \times \left\{ I_0(2\gamma_i \kappa \rho) - \cos \left[\frac{\gamma_r \kappa^2 (h-H_0)}{k_d \cos \Theta} \right] \right\}. \quad (8)$$

When $B_{I, down}(\rho, L)$ is calculated, it scarcely depends on ρ and is about 0.41, that is, the same as the log-intensity variance of a plane wave propagating along the downlink.

3. MEASURED OFF-AXIS BEAM ANGLE DEPENDENCE OF UPLINK FLUCTUATION

3.1 Experimental setting

A beam was transmitted from a ground station in Koganei, Tokyo, and received by an optical receiver carried on the ETS-VI satellite. The optical layout of the ground laser transmitter is shown in Fig. 3. The telescope for tracking the satellite was supported by a gimbal mechanism, and the laser transmitting telescope was installed on the side of the satellite tracking telescope. The beam expander was a Galilean type ($\times 2$), and the transmitting telescope had 10 times magnification, so the beam was transmitted with $W_0 = 0.055$ m. Table 1 shows the experimental conditions for the uplink transmission and the major settings of the ground transmitter and onboard receiver. The uplink intensity from the onboard receiver (CCD) was recorded at 1-second intervals.⁵ The direction of the uplink beam to the satellite was adjusted based on the uplink intensity measured by the CCD, and the off-axis beam angle dependence of the uplink intensity fluctuation was measured. On this account, we thought that the pointing error of the uplink was almost equal to 3 μrad (rms), which was the angular error in tracking the ETS-VI satellite with the satellite tracking telescope.

3.2 Uplink beam collimation

The beam was pointed at the satellite under the on-axis condition ($\langle \phi \rangle = 0$), and the focus of the beam expander was adjusted to collimate the beam. The uplink intensity, $I(0)$, was acquired while the focus was adjusted. The normalized intensity variance of $I(0)$ (variance of $I(0)$ over the square of $\langle I(0) \rangle$) as a function of $1/R_0$ is shown in Fig. 4. When $\langle I(0) \rangle$ had the largest value, we assumed the collimated state ($1/R_0 = 0$) and set the origin of the horizontal axis of Fig. 4. Each value of $1/R_0$ was calculated using the values of the space between two adjacent lenses of the beam expander. The normalized

intensity variance was minimum when $\langle I(0) \rangle$ was maximum.

3.3 Beam scanning and results

The uplink beam was scanned under the collimated condition ($1/R_0 = 0$) using the tip-tilt mirror in the ground laser transmitter. The step size of the scanning angle, ϕ_{scan} , was $4.0 \mu\text{rad}$ in the azimuth direction in the output space, and $2.6 \mu\text{rad}$ in the elevation direction. The beam was scanned at 1-minute intervals, and the intensity $I(\phi_{scan})$ of the beam received by the CCD was recorded. Figure 5 shows the time averaged $I(\phi_{scan})$ along the azimuth and elevation directions, and Fig. 6 shows the normalized intensity variance of $I(\phi_{scan})$ for each scan. The origin of the horizontal axis in Figs. 5 and 6 was set when $\langle I(\phi_{scan}) \rangle$ was maximum.

3.4 Discussion

The estimated irradiance of the uplink was 0.23 mW/m^2 at the peak of the beam pattern, when the uplink was transmitted under collimation conditions, W_0 was 0.055 m , atmospheric transmittance was assumed to be 0.64 , λ was $0.51 \mu\text{m}$, Θ was 26° , and atmospheric turbulence was assumed to be absent. This is about 18 times the measured value ($12.7 \mu\text{W/m}^2$) derived the result of $\langle I(\phi_{scan}) \rangle$. In the theoretically calculated off-axis beam angle dependence, shown in Fig. 1, the difference between the peaks of the two patterns at $\phi = 0$ was about 23 times. The measured results thus closely coincide with the theoretical one.

The beam divergence ($1/e^2$) for the results shown in Fig. 5 was about $40 \mu\text{rad}$ at full width for both scanning directions while for the results shown in Fig. 1 (the dotted curve) it was about $30 \mu\text{rad}$. This difference was apparently caused by a pointing error in the measurements.

When the atmospheric turbulence is in the weakly region, the normalized intensity variance of the intensity fluctuation is almost equal to the log-intensity variance.⁶ The results shown in Fig. 6 have a V-shaped variation, and the normalized intensity variance was minimum at $\phi_{scan} = 0$, similar to the theoretical calculation of the log-intensity variance. However, the variation rate of the measured normalized intensity variances was gradual compared with the theoretical results for $W_0 = 0.055 \text{ m}$ (the solid curve in Fig. 2). One reason for this difference is smoothing of the uplink variation due to the exposure time in the CCD. The uplink variation measured using another onboard receiver, which had a sampling rate higher than that of the CCD, indicated that the average coefficient of the normalized intensity variance received by the CCD was 0.2 .⁷ This averaging effect generally decreased the normalized intensity variance. The pointing error may be the result of a decrease in the measured mean intensity at the center of the beam

pattern and an increase in the intensity at the side of the pattern. Therefore, the rate of variation in the normalized intensity variance of $I(\phi_{scan})$ was smoothed. We plan to investigate this hypothesis quantitatively as future work.

The experimental results shown in Figs. 5 and 6 qualitatively agree with the theoretically calculated ones; the beam pattern was widened by atmospheric turbulence and the log-intensity variance increased with the off-axis beam angle. Transmitting a large divergence beam is the simplest way to avoid increasing the log-intensity variance; however, the irradiance would decrease as the divergence was increased. A more promising approach to reducing intensity fluctuation in an uplink is to transmit multiple beams using separate apertures.

4. CONCLUSION

The mean intensity and log-intensity variance of laser beam transmission as a function of the off-axis beam angle were theoretically calculated. We showed qualitative matching between the measured off-axis beam angle dependence of the uplink fluctuation and the theoretical one. In an uplink transmission experiment, the normalized intensity variance was minimum when the mean intensity was maximum when the wavefront curvature of the beam was varied.

REFERENCES

1. W. B. Miller and J. C. Ricklin, "Log-amplitude variance and wave structure function: a new perspective for Gaussian beams," *J. Opt. Soc. Am. A*, vol.10, 661–672, 1993.
2. J. D. Shelton, "Turbulence-induced scintillation on Gaussian-beam waves: theoretical prediction and observations from a laser-illuminated satellite," *J. Opt. Soc. Am. A*, vol. 12, 2172–2181, 1995.
3. L. C. Andrews and R. L. Phillips, *Laser beam propagation through random media* (SPIE Opt. Eng. Press, Bellingham) pp. 241–246, 1998.
4. L. C. Andrews, R. L. Phillips, and P. T. Yu, "Optical scintillations and fade statistics for a satellite-communication system," *Appl. Opt.*, vol. 34, 7742–7751, 1995.
5. K. Komatu, S. Kanda, K. Hirako, T. Ohashi, M. Shikatani, Y. Arimoto, and T. Aruga, "Laser beam acquisition and tracking system for ETS-VI laser communication equipment (LCE)," in *Free-Space Laser Communication Technologies II*, D. L. Begley and B. D. Seery, eds., Proc. SPIE 1218, 96–107, 1990.
6. V. I. Tatarski, *Wave propagation in a turbulent medium* (McGraw-Hill, New York) pp. 208–257, 1961.
7. M. Toyoshima and K. Araki, "Effects of time averaging on optical scintillation in a ground-to-satellite atmospheric propagation," *Appl. Opt.*, vol.39, 1911–1919 2000.

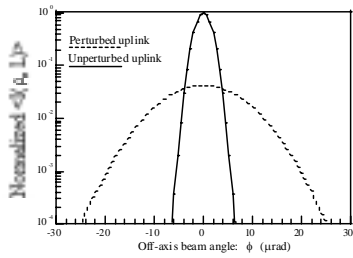


Fig. 1 Off-axis beam angle dependence of $\langle I(\rho, L) \rangle$ for atmospheric-perturbed and unperturbed uplinks for $W_0 = 0.055$ m.

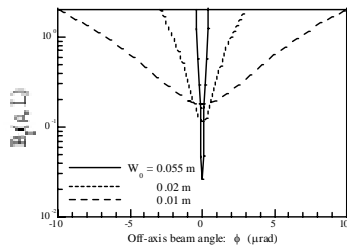


Fig. 2 Off-axis beam angle dependence of $B_I(\rho, L)$ of uplink calculated for $W_0 = 0.055, 0.02,$ and 0.01 m.

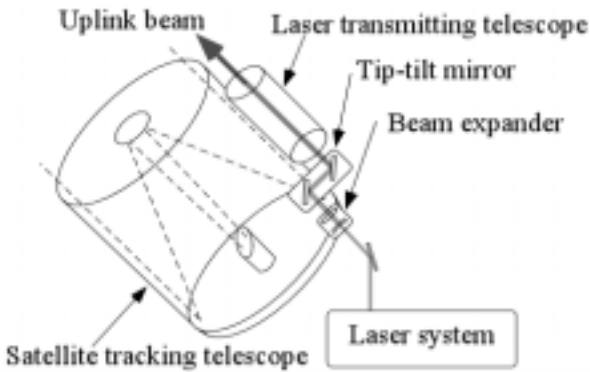


Fig. 3 Schematic of optical layout of ground laser transmitter.

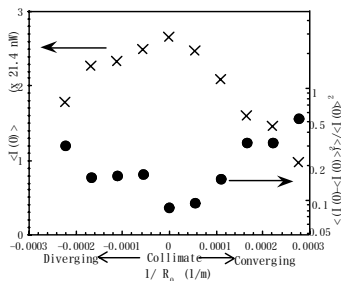


Fig. 4 Measured $\langle I(0) \rangle$ and normalized intensity variance of $I(0)$ (variance of $I(0)$ over square of $\langle I(0) \rangle$) as function of $1/R_0$.

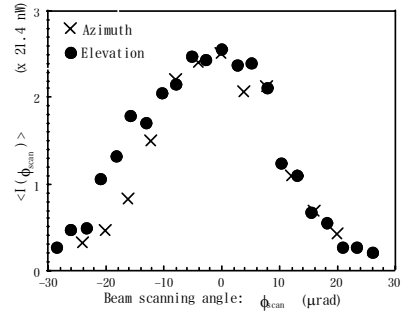


Fig. 5 Measured time averaged uplink intensity $\langle I(\phi_{scan}) \rangle$ as a function of beam scanning angle ϕ_{scan} in azimuth and elevation directions.

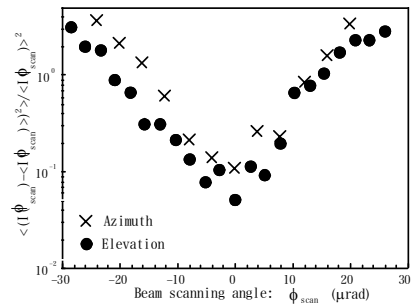


Fig. 6 Measured normalized intensity variance $\langle (I(\phi_{scan}) - \langle I(\phi_{scan}) \rangle)^2 \rangle / \langle I(\phi_{scan}) \rangle^2$ as a function of beam scanning angle ϕ_{scan} in azimuth and elevation directions.

Table 1 Experimental conditions for uplink transmission and major settings of ground transmitter and onboard receiver.

Time and date	23:57–24:36 Jan. 27–28 1996
Ground station point	35.7°N, 139.5°E, 122 m
Zenith angle: θ	25.7–26.5°
Range to satellite	37,400–38,500 km
Ground laser transmitter	
Wavelength	0.51 μm
Transmitting power	7.1 W
Beam radius	0.055 m
Satellite tracking error	3 μrad (rms)
Onboard optical receiver	
Aperture diameter	7.5 cm
Optical sensor type	CCD
Frame rate	30 s^{-1}
Data sampling interval	1 s